Journal of Materials Processing Technology 192–193 (2007) 83–88

Journal of Materials Processing Technology

www.elsevier.com/locate/jmatprotec

Investigations into the effects of electron beam welding on thick Ti–6Al–4V titanium alloy

N. Saresh [a], M. Gopalakrishna Pillai [b], Jose Mathew [a,*]

[a] Department of Mechanical Engineering, National Institute of Technology Calicut, NIT Campus P.O., Calicut 673601, Kerala, India
[b] Kerala Hitech Industries Limited, Beach P.O., Chakai, Trivandrum, Kerala, India

Abstract

Electron beam welding (EBW) of titanium alloy Ti–6Al–4V is not an easy task and finding the correct welding parameters is one of the critical activities when the product is intricate in shape. The procedure adopted to weld 17.5 mm thick joint in a spherical titanium gas bottle using EBW is presented here. Available EBW machine was capable of welding full penetration joint only up to 12.5 mm in titanium. Single sided partial penetration weld yielded poor result in production welding due to repeated defects like lack of fusion, root porosities, weld bead depression, under cut, etc. A two-pass double side welding technique was developed, and a joint thickness of 21 mm was decided so that a partial penetration weld can be attempted with lesser beam power. The extra material kept at the root of the weld can be machined off after welding. Single pass was made from one side of the joint producing a partial penetration weld with a penetration of nearly 19 mm. The second pass was made from the reverse side of the joint producing a similar partial penetration weld with almost the same penetration as that of the first weld. Trial welds were carried out and considerable difficulties were encountered in developing the welding procedure for establishing a defect free weld. Fusion zone voids and root porosities were observed and techniques were developed which eliminated their occurrence. Systematic weld qualification was carried out on coupon level and mechanical property and microstructure evaluations were carried out to ensure the joint integrity. Based on the technology developed and parameters arrived, the final specimen was welded. After passing through non-destructive tests, it was subjected to hydraulic proof pressure test with strain gauges and acoustic emission sensors for validating the capability of the technology developed. It has qualified all the test requirements as per the specifications and has been used for aerospace applications.

Keywords: Ti–6Al–4V; EBW; NDT; AE

1. Introduction

Titanium is a unique material, which requires special attention in all the areas of processing, especially in welding. Titanium and its alloys are available in various ranges of high specific strengths and are considered as one of the best engineering material for industrial application. The excellent combination of properties such as moderately high specific strength, high fatigue life, toughness, excellent resistance to corrosion and low density makes them attractive for aerospace applications. Titanium exists in two allotropic phases, α phase and β phase. The HCP structured α is stable up to 882 °C and transforms to BCC β thereafter. By properly alloying certain elements, α, near α, α–β, near β and β alloys can be produced. Ti–6Al–4V, which is a α–β titanium alloy is currently the 'work horse' titanium alloy of aerospace industry due to its good strength coupled with good fabricability [1]. It contains about 6% aluminium for α stabilization and 4% vanadium for β stabilization. This α–β alloy offers the possibility of varying mechanical and physical properties by the control of micro structural development during thermo-mechanical processing. The higher content of interstitial elements like oxygen and nitrogen gives slightly higher strength but lower ductility and toughness whereas, lesser content of these elements will improve ductility, fracture toughness, stress corrosion resistance and resistance to crack growth. The alloy containing low interstitial elements is generally called extra low interstitial or ELI grade [2]. The welding technology of titanium is complicated due to the fact that at temperatures above 550 °C, and particularly in the molten stage, it is known to be very reactive towards atmospheric gases such as oxygen, nitrogen, carbon or hydrogen causing severe embrittlement. Poor preparation and cleaning of the joint and filler materials before and during welding, poor shielding of the weld zone or impurities in the shielding gas can cause contamination [3–5].

* Corresponding author. Tel.: +91 9447416639; fax: +91 495 2287250.
E-mail address: josmat@nitc.ac.in (J. Mathew).

0924-0136/$ – see front matter © 2007 Elsevier B.V. All rights reserved.
doi:10.1016/j.jmatprotec.2007.04.048

Table 1
Chemical composition of Ti–6Al–4V plates

C	O	N	H	Fe	Al	V	Ti
0.01	0.152	0.009	0.003	0.004	6.17	4.07	Bal.

Table 2
Mechanical properties of the parent metal

UTS (MPa)	PS (MPa)	% Elongation
985	947	15

Titanium alloys may be joined by a variety of conventional and solid-state welding processes although its chemical reactivity requires special precautions to avoid contamination of the fusion and heat affected zone (HAZ) both on the face and root sides of the of the joint. Fusion welding of titanium is performed principally in inert gas shield and with high energy beam. Electron beam welding (EBW) is highly suited for joining titanium, as the high vacuum inside the chamber where the process is carried out, shields hot metal from contamination. Moreover, joint depth can be achieved with high beam power density and with lower heat input, when compared to arc welding processes [6,7].

Spherical titanium gas bottles are used in satellite launch vehicles for storing helium gas under very high pressure. These gas bottles are realized from hot formed and machined hemispherical dishes made out of Ti–6Al–4V. Machined adaptors are electron beam (EB) welded to these hemispherical dishes for gas entry and exit. These hemispherical sub-assemblies are closed together again by EB welding process. The development carried out for the EB welding of the 17.5 mm thick joint in a particular gas bottle is presented here [8]. The size of the gas bottles is 600 mm inside diameter with wall thickness of 11.2–17.5 mm. The joint thickness at the adaptor weld region is 17.5 mm and that at hemisphere to hemisphere is 12.2 mm. Such bottles are designed to withstand a maximum expected operating pressure (MEOP) of 330 bar. To develop the EB welding parameters the material used was 21 mm thick Ti–6Al–4V plate, conforming to ASTM –B265 grade-5 in hot rolled and mill-annealed condition. The microstructure of the plate was characterized as fine equiaxed $\alpha + \beta$ structure. Chemical composition and mechanical properties of these plates are given in Tables 1 and 2, respectively.

2. Experimental work

100 mm × 150 mm test plates were welded to make weld coupons of size 200 mm × 150 mm size. The edges of the test plates were carefully machined to obtain a perfect square-butt joint for EBW. The welding was carried out on a 15 kW high voltage EBW machine; Dynaweld Xw150.15. The welding parameters were arrived at in three phases viz.: phase-0, phase-1 and phase-2.

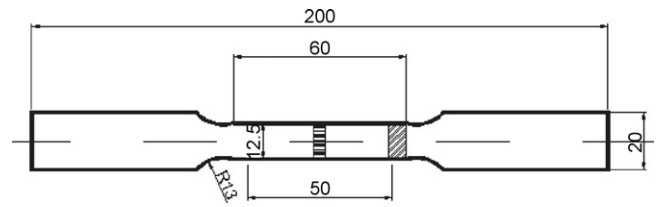

Fig. 1. Tensile test specimen [ASTM A 370, all dimension is in mm].

In phase-0, many bead-on trials were done to get the ideal weld parameters and to attain satisfactory bead formation. Initially, the trials were started with the thickness of 17.5 mm, but could not succeed in achieving a satisfactory full penetration joint. With certain set of parameters, under bead spraying was observed with sinking of the top bead. When the beam power was increased, the penetration became excessive and uneven drops of weld metal globules were found in the root side due to the lower surface tension of the titanium metal. Trials were done adopting various parameters with reduced speed and changing the focusing pattern of the beam, but the results were not satisfactory. The available capacity of the machine was not enough to form a keyhole in 17.5 mm thick titanium material. In the absence of keyhole in EBW, the under bead cannot form and full penetration weld was not possible. Since numerous attempts failed to produce a satisfactory full penetration joint in 17.5 mm thickness, attention was diverted for a partial penetration joint on a higher thick material so as to ensure a minimum penetration of 19 mm. So a joint thickness of 21 mm was decided so that the excess material of 3.5 mm kept at the root side of the weld can be machined off after completing the weld.

2.1. Single pass partial penetration welding of 21 mm thick joint

The phase-0 bead-on trials were repeated on 21 mm thick plate for a partial penetration joint aiming for a minimum penetration of 19 mm. In this case also difficulties were encountered in achieving a good weld metal root. With a certain set of parameters, lack of fusion was observed but when the beam power was slightly increased, characteristic drops of weld metal globules were formed in the root with an excessive top bead sinking. After a series of trials, a set of parameters were arrived at, this resulted in a just penetrating condition with satisfactory top bead.

With these parameters, phase-1 development was started on plate joints. Weld parameter was further fine-tuned in this phase to get a satisfactory weld with a good top bead and just root fusion condition as explained above. After radiography test and fluid penetrant test (as per ASTM E165-02), tensile testing and microstructure evaluation of these welds were conducted [9]. The tensile test specimen used as per ASTM A 370 is shown in Fig. 1.

The phase-2 developments were done on circular disc joint simulating the actual joint configuration. In this phase also technical difficulties were encountered on the overlap region. The diameter of the joint was 80 mm. The localized residual heat generated at the slope-in region caused the net amount of input heat in the overlap area to increase considerably, resulting in top bead undercut and also formation of weld metal globules at the root as shown in Fig. 2.

By adjusting the slope-in/slope-out rates and slightly varying the parameters, these problems were solved and a satisfactory weld in the simulated condition was obtained as shown in Fig. 3. The finalized parameters are given in Table 3. With these parameters, a batch of actual product was welded in a single campaign. Post machining fluid penetrant test at the root side of the weld revealed chain porosities at some discrete locations. This was probably due to the entrapped shrinkage porosities at the root, which might have opened up during machining. Finally this was sealed off with a low power sealing run weld in EBW

Table 3
Weld parameter for 21 mm single pass partial penetration weld

Voltage (kV)	Beam current (mA)	Focusing current (mA)	Welding speed (mm/min)	Slope-in rate (mA/s)	Slope-out rate (mA/s)	Gun to work distance (mm)	Heat input (kJ/cm)
140	75	675	1270	5.8	6.0	370	4.96

(a)

(b)

Fig. 2. Circular weld (a) with top bead undercut, (b) with weld metal globules at the root.

from the root side. However, during the second batch of welding, repeatability could not be achieved and resulted in lot of rejection due to lack of fusion (LF), porosity, top bead sinking, etc. This was due to the fact that the fixed parameters were so sensitive that even a marginal reduction in heat input caused LF, where as a marginal increase in beam power resulted in top bead undercut [10,11].

2.2. Two-pass, double side welding of 21 mm thick joint

A two-pass, double side welding technique was further developed for welding 21 mm thick joint to overcome this situation. One pass was made from one side of the joint producing a partial penetration weld with a depth of penetration exceeding 50% of the joint thickness. The second pass was made from the reverse side of the joint by employing the same beam power as that of the first weld. The position during welding is shown in Fig. 4. The tensile specimens

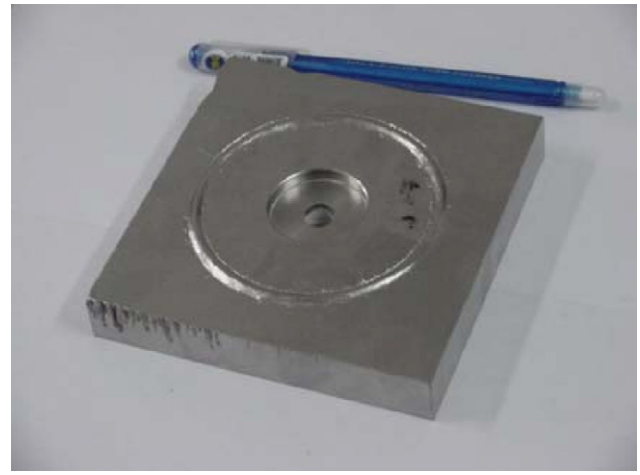

Fig. 3. Good circular weld.

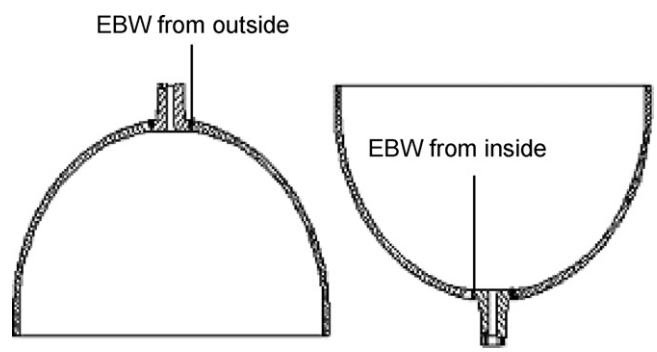

Fig. 4. Double side weld set-up.

prepared from this weld failed due to inter-pass lack of fusion. On analysis it was revealed that the second pass was not penetrated up to 50% thickness due to higher gun-to-work distance. Therefore, another set of parameters were arrived, which ensured penetration up to 19 mm on either side so that both welds will be sufficiently over lapping each other and ensuring full elimination of lack of fusion. The parameters thus derived for double side welding are given in Table 4.

Tensile properties and microstructure were evaluated, which were meeting the requirements. With this set of parameters, a simulated ring joint was welded from both sides with the same slope-in/slope-out rates as fixed in single sided weld. This weld was totally acceptable in visual, NDT and in microstructure studies. Thus the welding process was frozen and the welding process specification (WPS) document was prepared.

Having attained the confidence in two-pass double side EB welding of 21 mm joint, a batch of hemispherical domes was welded with adaptors. Fusion zone voids were observed in X-ray radiographs of few welds, which were repaired by giving one more weld from the reverse side of the joint. The occurrence of these voids was due to weld joint contamination as a result of delay in carrying out the second side weld. This was solved by carrying out the second side welding on the same day itself by suitably modifying the fixture to accommodate change in set-up without difficulty. With this change, another batch was welded and these welds were totally accepted. Another notable point in this case is that there were no porosities observed during the post machining fluid penetrant test of

Table 4
Weld parameter for 21 mm two-pass double side weld joint

Voltage (kV)	Beam current (mA)	Focusing current (mA)	Welding speed (mm/min)	Slope-in rate (mA/s)	Slope-out rate (mA/s)	Gun to work distance (mm)	Heat input (kJ/cm)
140	65	675	1270	5.8	6.0	370	4.3
140	65	638	1270	5.8	6.0	600	4.3

Fig. 5. Pressure test set-up.

these weld joints. After passing through the NDT checks, the final product was proof pressure tested at 495 bar (1.5 times the MEOP) with strain gauges and acoustic emission (AE) sensors. The test set-up is shown in Fig. 5. There were no unusual signals from AE sensors and the strain values were lower than the predicted values and the process capability is ensured. Hence the welding could be done continuously on production mode with out any problem.

3. Results and discussions

The mechanical properties of single sided 21 mm weld obtained are given in Table 5. The specimen thickness was reduced to 17.5 mm by removing material from the root side of the weld and the testing was done by retaining the top bead. The minimum values required as per standards is 920 MPa ultimate tensile strength (UTS), 840 MPa, 0.2% proof stress (PS) and 10% elongation. From Table 5, it can be seen that all the values are above the requirements. Average weld joint efficiency of this weld considering the parent metal strength from Table 2 is 97.5% in UTS, 95.3% in PS and 79.8% in elongation. The reduction in UTS and PS value is due to the fact that there is a transition from equiaxed to an acicular microstructure. The ductility of the welded sample is low compared to that of the parent metal. This low ductility is attributed to the microseggregation which occur during the solidification of the weld pool. Microseggregation results in non-uniform hardening and embrittlement [12,13]. These results confirm the acceptability of the weld for indented use, considering the strength.

Mechanical properties of two-pass double side welding obtained are given in Table 6. The properties of a set of specimens tested with different conditions are given. To understand the variation of properties at the middle of the section due to overlapping effect of two welds, specimens were machined equally from both sides and reduced the thickness to 10 mm and tested. Similarly, specimens were taken from top of the section by removing 3.5 mm material from the second side-welded portion keeping the thickness to 17.5 mm. From the values reported in Table 6, it can be seen that there is no variation in properties with respect to overlapping effect of the two welds. All the values in Table 6 are well above the standard requirements except for stray cases of lower elongation due to reasons explained later. Average weld joint efficiency of this weld considering the parent metal strength

Table 5
Mechanical property of 21 mm single pass partial penetration weld

Specimen no.	UTS (MPa)		0.2% PS		% of elongation	
	Values	Average	Values	Average	Values	Average
1	96		913		11.2	
2	97	96.33	910.7	911.2	12	11.7
3	96		910		12	

Table 6
Mechanical properties of 21 mm, two-pass double side weld

Batch	UTS (MPa)		0.2% P.S		% Elongation		Condition of specimen	Remarks
	Values	Average	Values	Average	Values	Average		
1	970 968 963	967	922 924 919.8	921.9	13 9.8* 6.5*	9.7	Top bead retained, thickness reduced to 17.5 mm	* Failed at weld edge due to notch effect
2	979 971 973	974.3	930 926 927	927.6	11.9 12.2 12	12	Top bead removed, thickness reduced to 17.5 mm	Re-test after top bead removal
3	994 984 985	987.6	943 928 930	933.6	11.2 11.2 12.2	11.5	Top bead retained, thickness reduced to 17.5 mm	Re-welded specimen without notch
4	987 976 980	981	932.7 936.4 936.4	935.1	11.2 11 12	11.4	Specimen thickness 10 mm	Middle section properties

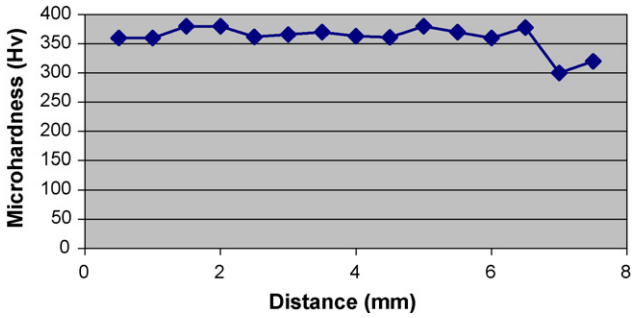

Fig. 6. Microhardness across PM, HAZ and weld.

from Table 2 is 99% in UTS, 97.2% in PS and 79.4% in elongation. From this result, it can be inferred that the UTS and the PS are better than the previous case of single sided weld. There is an increase of 1.5% in UTS and 1.9% in PS of two-pass double side welding compared to single pass weld.

The microhardness in Vickers scale across the weld is also mapped and is given in Fig. 6, which shows that the hardness is marginally higher in the weld fusion zone and HAZ as compared to the parent metal. The average increase of hardness in HAZ is 37 HV and in fusion zone is 34 HV as against the parent metal hardness of 335 HV.

Another observation from Table 6 is that two of the specimens in the top bead retained condition failed with a low elongation of 9.8 and 6.5%. These specimens were broken at the weld edge without appreciable necking. The photograph of one of this specimen is given in Fig. 7 along with a normally broken specimen with good neck formation. The crack in the less elongated specimen has initiated from the root of a small notch on the weld edge. The specimens from the same batch, machined from both sides showed good elongation with appreciable neck formation and none of the specimens failed with elongation less than 10%. Another set of specimens taken from a different coupon welded without notch by marginally adjusting the weld parameters also showed good elongation with appreciable neck formation. So it can be inferred that the notches or side undercuts in EB welds are acting as stress raisers resulting in brittle failure with low elongation. Therefore the side undercuts in EB welds are to be either

Fig. 7. Broken specimens.

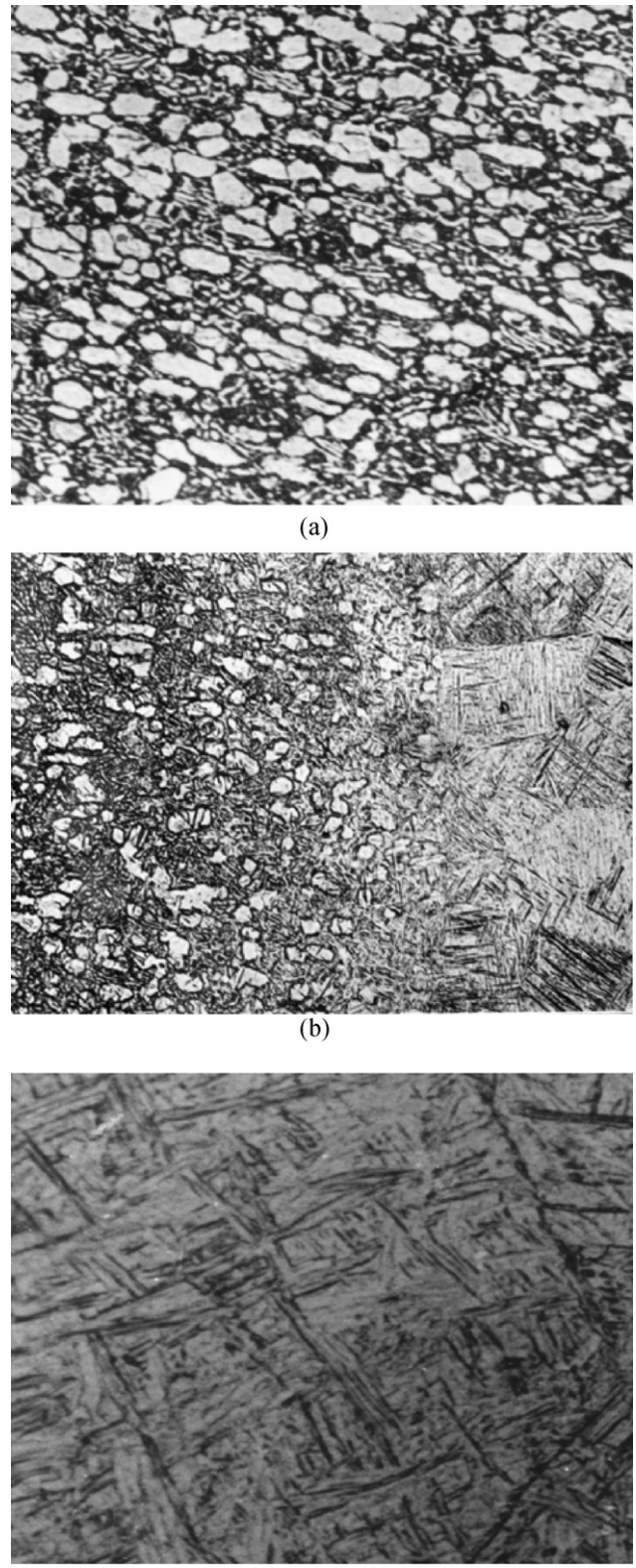

Fig. 8. Microstructures: (a) microstructure of parent metal (×320), (b) microstructure of parent metal, heat affected zone and fusion zone (×320), (c) microstructure of fusion zone (×320).

eliminated by employing suitable weld parameters or made less severe by cosmetic welding.

Microstructure of parent metal, HAZ and fusion zone is given in Fig. 8. Microstructure characterization of the joint shows transition of microstructure from an equiaxed to an acicular microstructure. This variation is due to melting of the base metal during welding and subsequent cooling with a different cooling rate [14]. Different microstructure can be seen for parent metal, HAZ and fusion zone due to different rate of cooling.

4. Conclusions

From the extensive studies conducted, the following conclusions were drawn.

1. Full penetration single pass EB weld joint is not possible for 17.5 mm thick titanium due to constraints in the available EB welding machine.
2. Single sided partial penetration joint for 17.5 mm thick titanium joint failed to produce consistent welds due to lack of repeatability of weld parameters during production welding.
3. Two-pass double side welding can be adopted for welding of 17.5 mm thick titanium joints. The mechanical properties are higher and consistent throughout the weld cross section. The microhardness is almost uniform across the parent metal, HAZ and the weld fusion zone. The microstructure is comparable with that of a normal full penetration EB weld.
4. The reverse side welding is to be completed as early as possible to eliminate fusion zone voids due to weld joint contamination.
5. Side undercuts acts as stress raisers, which is detrimental to a pressure vessel and hence is to be eliminated or reduced. Ensuring proper selection of weld parameters can eliminate this factor. However once it occurs, employing an additional cosmetic weld can reduce the effect. This possibility can be fully eliminated by providing machining stock on both sides and by introducing post weld machining on either side.

References

[1] R.R. Boyer, An overview on the use of titanium in the aerospace industry, Mater. Sci. Eng. A 213 (1996) 103–114.
[2] M.J. Donarchie Jr., Titanium—A Technical Guide, ASM International, 2000.
[3] Welding Hand Book, vol. 2, Welding Processes, AWS, 1988, pp. 695–697.
[4] Welding Hand Book, vol. 4, Metals and Their Weldability, AWS, 1982, pp. 447–449.
[5] B. Gupta, Aerospace Materials, vol. 1, S-Chand and Company Ltd., New Delhi, 1996.
[6] J.L. Barreda, F. Santamaram, X. Azpiroz, A.M. Irisarri, J.M. Varona, Electron beam welded high thickness Ti–6Al–4V plates using filler material of similar and dissimilar composition to the base metal, Vaccum 62 (2001) 143–150.
[7] W.A. Baeslack, D.W. Becker, F.H. Froes, Advances in titanium alloy welding metallurgy, J. Metals 36 (1984) 46–58.
[8] N. Saresh, Investigations into the effects of EBW and GTAW on Ti–6Al–4V titanium alloy, M.Tech. Thesis, Department of Mechanical Engineering, NIT Calicut, Kerala, India, 2005.
[9] Standard Test Method for Liquid Penetrant Examination, ASTM Standards, E 165-02 (2002) 1–20.
[10] Qi. Yunilian, Deng Ju, Hong Quan, Zeng Liying, Electron beam welding, laser beam welding, gas tungsten arc welding of titanium sheet, Mater. Sci. Eng. A 280 (2000) 177–181.
[11] W.K.C. Yung, An investigation of the welding parameters affecting the tensile properties of titanium welds, J. Mater. Process. Technol. 63 (1997) 759–764.
[12] M.A. Green Field, D.S. Duvall, Welding of advanced high strength titanium alloy, Weld. J. 54 (1975) 73–80.
[13] R. Ding, Z.X. Guo, A. Wilson, Microstructural evolution of a Ti–6Al–4V alloy during thermo-mechanical processing, Mater. Sci. Eng. A 327 (2002) 233–245.
[14] R.C. Picu, A. Majorell, Mechanical behavior of Ti–6Al–4V at high and moderate temperatures. Part II. Consecutive modeling, Mater. Sci. Eng. A 326 (2002) 306–316.